J Solid State Electrochem (2010) 14:51–56
DOI 10.1007/s10008-009-0787-4

ORIGINAL PAPER

Effect of fullerene coating on silicon thin film anodes for lithium rechargeable batteries

Arenst Andreas Arie · Wonyoung Chang · Joong Kee Lee

Received: 10 September 2008 / Revised: 2 January 2009 / Accepted: 9 January 2009 / Published online: 24 January 2009

Abstract To improve the electrochemical performances of Si thin film anodes for lithium rechargeable batteries, fullerene thin films are prepared by plasma-assisted evaporation methods to be used as coating materials. Analyses via Raman and X-ray photoelectron spectroscopy indicate that amorphous polymeric films originated from fullerene are formed on the surface of the silicon thin film. The electrochemical performance of these fullerene-coated silicon thin film as an anode material for rechargeable lithium batteries has been investigated by cyclic voltammetry, charge/discharge tests, and electrochemical impedance spectroscopy. The fullerene-coated Si thin films demonstrated a high specific capacity of above 3,000 mAh g^{-1} as well as good capacity retention for 40 cycles. In comparison with bare silicon anodes, the fullerene-coated silicon thin film showed superior and stable cycle performance which can be attributed to the fullerene coating layer which enhances the Li-ion kinetic property at the electrode/electrolyte interface.

Keywords Lithium battery · Fullerene · Coating · Silicon thin film · Anodes

Introduction

Recently, rechargeable lithium batteries have become the main energy storage systems for a wide range of applications from mobile electronics to high-powered electric vehicles [1–3]. The demand for the batteries with higher capacity has increased in order to meet future demand [4, 5]. Consequently, alternative materials for high-capacity rechargeable lithium batteries have become one of the most important subjects for many research groups working in the field of electrochemistry [6, 7]. For anode materials, rechargeable lithium batteries still rely on conventional graphite materials which only give a limited capacity of about 372 mAh g^{-1}[8]. Based on its theoretical capacity of 4,200 mAh g^{-1}, silicon is promising material to replace the graphite as the anode materials for rechargeable lithium batteries [9, 10]. Unfortunately, there are some drawbacks that need to be addressed before introducing silicon as a commercial anode material. During the charging and discharging processes of lithium batteries, the silicon anodes exhibit a large volume increase about 300% due to the extraction/insertion of lithium ions which leads to the mechanical disintegration of the silicon material [11, 12]. This mechanical disintegration gives a drastic fading in the capacity even in the first few cycles because of the loss of electrical contact and cell failure [13, 14]. Especially for silicon thin film batteries, many attempts have been made to modify the surface property. One approach is to synthesize multilayered Si thin films with metal such as Al, Fe, and Cu nanodots [15–17] in order to compensate the effect of the volume expansion. In this paper, fullerene-coated silicon thin films have been synthesized by radiofrequency (RF) plasma-assisted deposition techniques. It is expected that fullerene films could act as a buffer layer to reduce the effect of the volume expansion during repeated cycling tests as well as to improve the Li-ion kinetic property at the interface of the Si electrode and the electrolyte. Fullerene has been used in previous experiments to coat the lithium metal anode, and significant improvements in the electrochemical performances have been reported [18].

A. A. Arie · W. Chang · J. K. Lee (✉)
Advanced Energy Materials Processing Laboratory,
Battery Research Center,
Korea Institute of Science and Technology,
P.O. Box 131, Cheongryang,
Seoul 130-650, Korea
e-mail: leejk@kist.re.kr

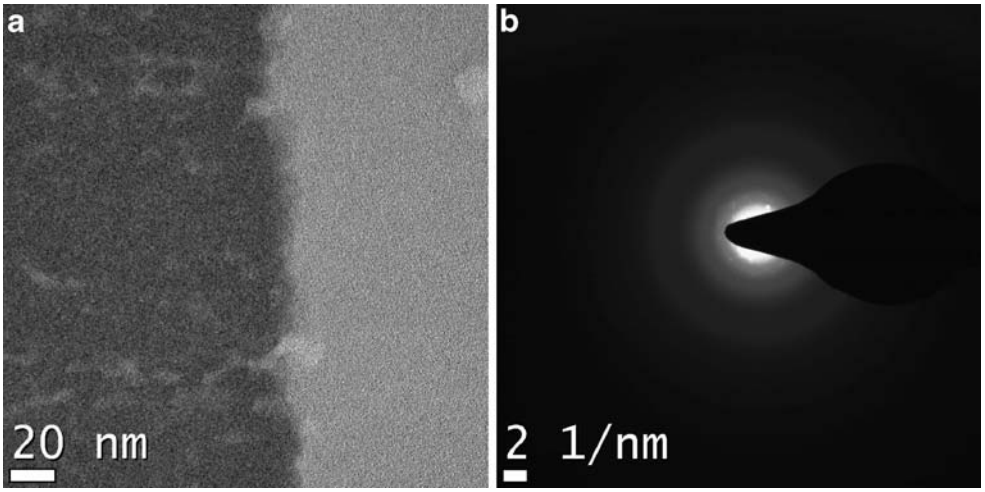

Fig. 1 High-resolution transmission electron microscope *HRTEM* image of interface between Si and fullerene films **a** and the selected area electron diffraction *SAED* patterns of fullerene coated silicon films **b**

Experimental investigations

Deposition of thin films

For the first step, silicon thin films are deposited onto 2×2-cm^2 copper foil with thickness of 2×10^{-5} m using radio frequency coupled plasma-enhanced chemical vapor deposition techniques under plasma power of 200 W with the base pressure at 1.5×10^{-5} Torr and the working pressure of 8.0×10^{-2} Torr controlled by an argon flow rate of 30 sccm. The silane gas is used as the precursor with a constant flow of 10 sccm, while the substrate temperature is 150 °C. Plasma assists the thermal evaporation technique and is then carried out to deposit fullerene films onto the silicon thin film. Initially, the evaporation chamber is evacuated down to the base pressure of 1.0×10^{-5} Torr using the rotary and turbo pumps. As the precursor to the carbon deposition, fullerene powder is initially put in the evaporation boat inside the evaporation chamber and silicon thin film is prepared as the substrate to be coated. The deposition of fullerene films is then conducted at the working pressure of 1×10^{-2} Torr under an argon gas flow of 30 sccm and RF plasma power of 100 W. The fullerene powder is then vaporized and deposited on the silicon thin film substrate. During the deposition of fullerene thin films, the substrate temperature is maintained at 150 °C. For the determination of specific capacity of the thin film electrodes, the amounts of active material were calculated as follows:

$$z = x - y,$$

where z(in g) is the amount/weight of active materials, x(in g) is the total weight of 2×2-cm^2 thin film anode foil after thin film deposition, and y(in g) is the weight of corresponding 2×2-cm^2 bare copper foil before thin film deposition.

From this procedure, the average mass density mass per square area of active material is about 0.1 mg cm^{-2}.

Characterization of the thin films

The morphology and structural property of the thin films, especially the fullerene films, have been observed by

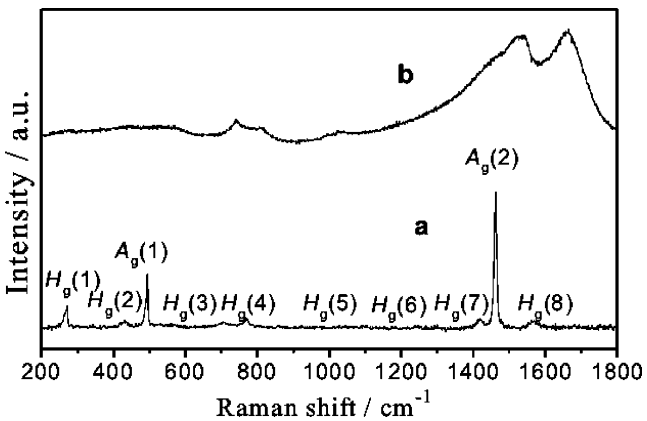

Fig. 2 Raman spectra of un-polymerized fullerene sample (**a**) and polymerized fullerene films deposited on the surface of silicon thin film anodes (**b**)

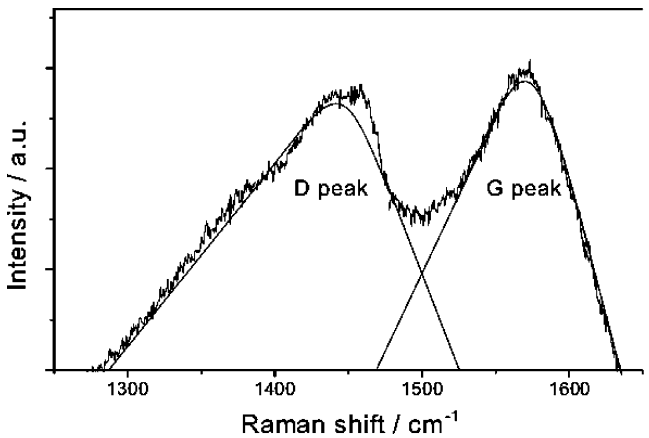

Fig. 3 Deconvolution of Raman spectra for polymerized fullerene thin films deposited on the surface of silicon thin film anodes

Table 1 Parameters of the Raman spectra deconvolution

D peak frequency (cm^{-1})	1,432.87
FWHM D peak	131.5
G peak frequency (cm^{-1})	1,579.68
FWHM G peak	105.3
I_D/I_G	1.116

scanning electron microscope SEM, Hitachi equipped with energy-dispersive X-ray EDX spectroscopy, high-resolution transmission electron microscopes HRTEM, JEOL, Japan, Raman spectroscopy Nicolet Almega XR Dispersive Raman Spectrometer, Thermo Electron Corporation, USA with the 633-nm line of Ar laser, and X-ray photoelectron spectroscopy VG Scientific ESCALAB 200R, respectively. The electrochemical properties of thin film electrodes have been examined using a half cell. The cell consisted of the deposited thin film Si or fullerene-coated Si films on the copper foil as the working electrode and lithium metal foil as the counter electrode. The electrolyte is 1 M $LiPF_6$ in a mixture of ethylene carbonate, ethyl methyl carbonate, and dimethyl carbonate 1:1:1 by volume. The cells are then charged and discharged at constant current density of 0.1 mA cm^{-2} or about 0.33 C rate for specific capacity of 3,000 mAh g^{-1} and average mass density of 0.1 mg cm^{-2} with cutoff voltage of 0–2 V vs Li/Li^+ Maccor Series 4000 under room temperature. The cells were also tested for electrochemical impedance spectroscopy Zahner IM 6, amplitude of 5 mV and frequency range between 0.01 and 10^6 Hz and cyclic voltammetry CV measurements with a scan rate of 0.05 mV s^{-1}. The SEM images after the cycle tests are also taken to observe the evolution of the surface morphology.

Results and discussion

Figure 1a shows the HRTEM image of the interface between the silicon and fullerene thin films deposited on the silicon substrate; a clear contrast can be observed between these two layers. The selected area electron diffraction pattern see Fig. 1b shows very dispersed and weak diffraction rings. All of those observations indicate the amorphous nature of the thin films.

Figure 2 displays the Raman spectra of the un-polymerized/pristine fullerene and polymerized fullerene film deposited on the surface of the silicon thin film anodes. As can be seen, the Raman spectrum of the un-polymerized C_{60} sample contains ten peaks including the eight H_g modes and the two A_g modes. In the case of polymerized fullerene films, its Raman spectrum show new peaks due to the splitting of the original peak especially around the pentagonal pinch $A_g(2)$ mode at 1,469 cm^{-1}. This implies a lowering of molecular symmetry through the formation of covalent bonds between the fullerene molecules [19, 20)]. For quantitative analysis, the Raman spectra of the polymerized fullerene films have been fitted to the two peaks denoted G (graphite structure) and D (disordered graphite-like structure) peaks using a combination of Gaussian–Lorentzian bands [21, 22] as shown in Fig. 3. These D and G peaks are relayed with the structural and physical properties of carbon [23]. The parameters of the Raman spectra deconvolution of each peak are presented in Table 1; these include the full-width at half-maximum (FWHM) and the intensity ratio (I_D/I_G) which gives some information about the film's structure [24]. It can be seen from Table 1 that the FWHM value for the D band is larger than that for the G band, which reveals that more disordered carbon are found than in the graphite carbon as confirmed by the value of intensity ratio I_D/I_G (1.116) [25]. In conclusion of this Raman study, it can be said that the carbon films are in the polymerized state and mainly consist of disordered graphitic structure.

Figure 4 presents the X-ray photoelectron spectroscopy (XPS) spectra of C 1s for the un-polymerized and polymerized fullerene thin films on the surface of the Si film electrodes. The C 1s binding energies of the un-polymerized fullerene film and its polymerized film are determined to be 284.09 eV, which correlates with Vasquez's value of fullerene C_{60} [26, 27]. The FWHM of C 1s for the polymerized fullerene films increased to 1.63 eV compared with that of un-polymerized films (0.96

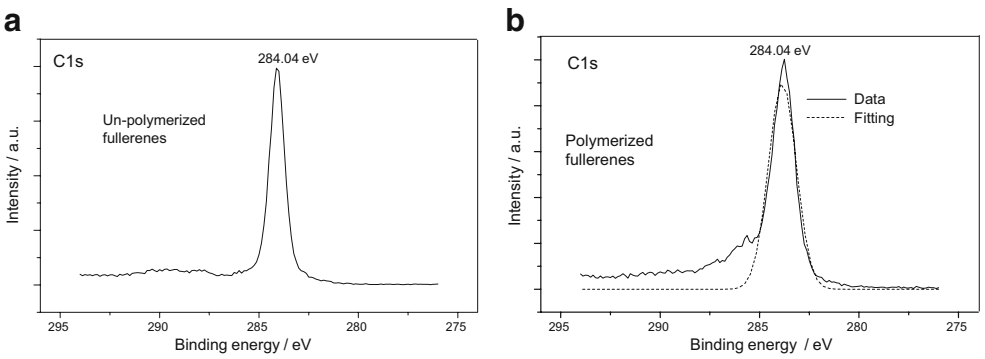

Fig. 4 C 1s X-ray photoelectron spectra of un-polymerized fullerene sample (**a**) and polymerized fullerene films on the surface of silicon thin film anodes (**b**)

eV). This high FWHM value and broader spectrum of the polymerized films indicates that the linking among the fullerene molecules has taken place during the deposition process [26, 27].

Figure 5 shows the CV curves of bare Si and fullerene-coated silicon thin films after first scanning the cycle obtained at a scan rate of 0.05 mV s^{-1}. In the case of bare Si thin film electrodes, the cathode peaks at about 0.5/0.3 V and anodic peaks at 0.25/0.03 V for Si–Li alloying/de-alloying reactions are observed. Both CV curves (for Si and fullerene-coated silicon electrodes) are quite similar with only the peak shifting observed for the fullerene-coated silicon case, revealing that the fullerene layer is an inactive layer with respect to the intercalation/de-intercalation of lithium ions into the silicon host matrix. The different surface film structure and composition may be the main factors causing this kind of peak shifting. In other words, the alloying/de-alloying reactions between the Li ions and the silicon are not affected by the presence of the fullerene layer since the basic reaction mechanism (alloying and de-alloying) is conserved. In addition, we can observe that under the same scan rate and voltage range, the fullerene-coated silicon films give a slightly lower current than that obtained by the bare Si films.

Figure 6 gives the cycling performance for bare Si film and for fullerene-coated Si film electrodes with a thickness of about 300 nm at current density of 0.1 mA cm^{-2}. We can see that the silicon film anode showed very poor cyclic performance due to the effect of the huge volume expansion. The initial capacity of both films is about 3,000 mAh g^{-1}, but the bare Si film shows rapid capacity fading due to the volume expansion effect; its capacity is about 500 mAh g^{-1} after the 40th cycle (with a capacity retention of 16.7%). On the contrary, the fullerene-coated silicon film maintained its high capacity even after the 40th cycle; its capacity remains about 3,000 mAh g^{-1}. The cyclic profile of the fullerene-coated Si thin film seems more

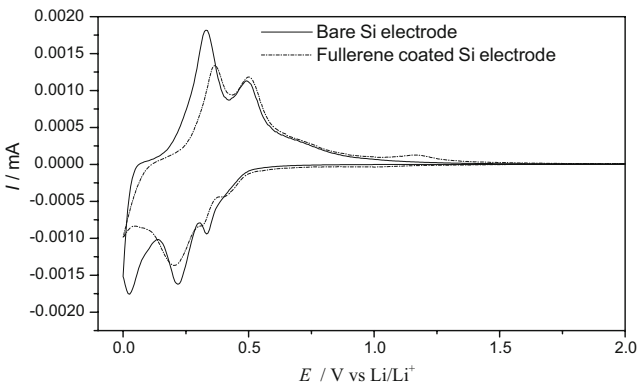

Fig. 5 Cyclic voltammetry (*CV*) of bare Si thin film and fullerene-coated Si thin film electrodes at a scan rate of 0.05 mV s^{-1}

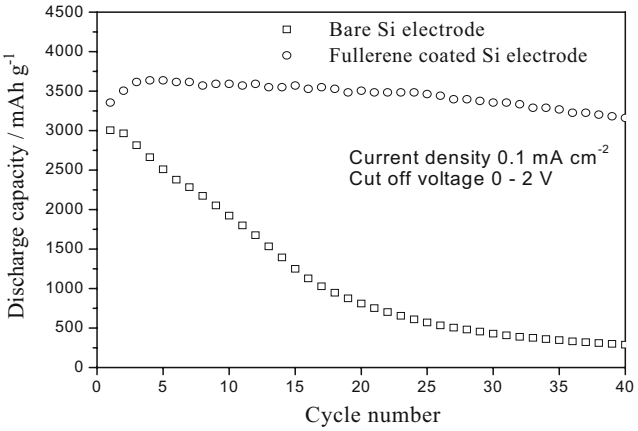

Fig. 6 Cycle performance of bare Si thin film and fullerene-coated Si thin film electrodes at current density of 0.1 mA cm^{-2}

stable during the cycle testing. The presence of the fullerene layer as a polymerized phase could be the essential factor enhancing the cyclic performance of the fullerene-coated silicon film electrodes. It seems that the effect of the volume expansion can be reduced in the case of fullerene-coated silicon film since the fullerene film acts as a passive layer protecting the silicon thin film against the side reaction with the electrolyte. For further confirmation, an electrochemical impedance measurement has been conducted for both thin film electrodes.

Figure 7 shows the electrochemical impedance spectra of bare Si thin film and fullerene-coated silicon thin film after the first cycle. The semicircle in the high-frequency range indicates the migration process of the Li ions through the surface film on the surface of the electrode, and the semicircle in the medium frequency range shows the charge transfer process at the electrode/electrolyte interface. As can be seen, the silicon thin film electrodes

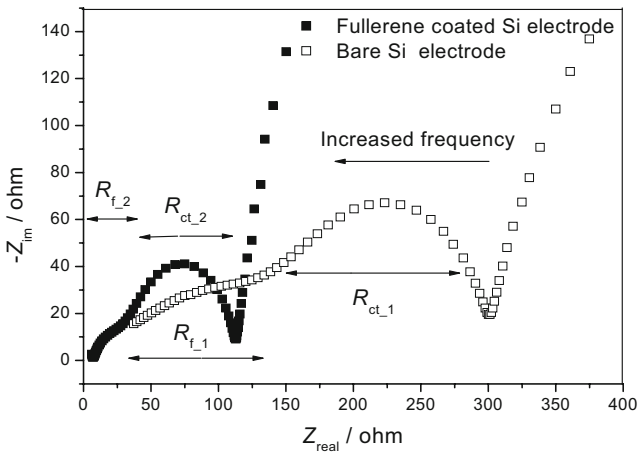

Fig. 7 Electrochemical impedance spectroscopy (*EIS*) plots of bare Si thin film and fullerene-coated Si thin film electrodes

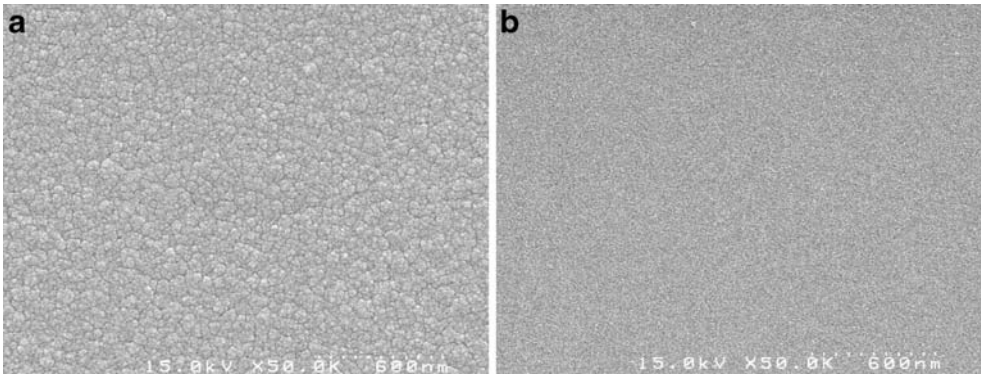

Fig. 8 Scanning electron microscope (*SEM*) images of as-deposited bare Si films (**a**) and fullerene-coated Si films (**b**)

displays the larger impedance compared with the Si/fullerene electrodes (larger diameter of the semicircle). It is already known that the volume expansion of the silicon host matrix caused by the alloying/de-alloying reactions between the lithium ions and the silicon such that the silicon surface can interact directly with the decomposed electrolyte. Therefore, the impedance of the silicon thin film is large due to the formation of the continuous formation of the solid electrolyte interphase (SEI) layer [28]. However, this undesired phenomena is not found in the case of fullerene-coated Si film anodes, as observed in Fig. 7; its impedance is much smaller since it could provide more surface stability against the side reactions with the electrolyte. For simple analysis, the resistance at the electrode/electrolyte interface can be decomposed into two major parts, namely the surface film resistance (at high frequency range) and charge transfer resistance (at middle frequency range) [29, 30]. As seen qualitatively from Fig. 7, in the case of bare Si electrode, its higher value of surface film resistance (R_{f_1}) is caused by the direct contact with electrolyte such that the more amounts of electrolyte decomposition occur and the unstable SEI film is formed on the surface of bare Si electrode. It is then followed by its high charge transfer resistance (R_{ct_1}) since the unstable SEI film makes the charge transfer process more difficult [28]. For the fullerene-coated Si electrode, it demonstrates lower resistance both for the surface film (R_{f_2}) resistance and charge transfer resistance (R_{ct_2}). So it is apparent that the fullerene layer can contribute to the formation of more stable SEI layer at the electrode/electrolyte interface since it prevents the decomposed electrolyte to have a direct contact with the Si electrode. Based on those findings, it can be concluded that the fullerene film contributes to the enhanced kinetic property of Li insertion/extraction into the silicon thin film anodes since it can suppress the side reaction between electrode and the electrolyte as well as provide a favorable path for Li-ion transfer.

Figure 8 shows the SEM images of as-deposited Si thin films (Fig. 8a) and fullerene-coated silicon films with fullerene film on the top layer (Fig. 8b). The fullerene film shows smaller size of agglomerates compared with that of Si films. Additionally, from cross-sectional SEM and EDX results (not shown here), the thickness of the films was about 300 nm and the atomic ratio and weight ratio of carbon (fullerene) were 2.8% and 6.4%, respectively. Figure 9 compares the SEM images of bare Si thin film and fullerene-coated silicon thin film after 30 cycles of repeated charging/discharging tests. From Fig. 9, it is clear that the surface of Si thin film suffers from large cracks, and eventually, these cracks causes the rapid capacity fading as shown in Fig. 6. On the other hand, the fullerene-coated

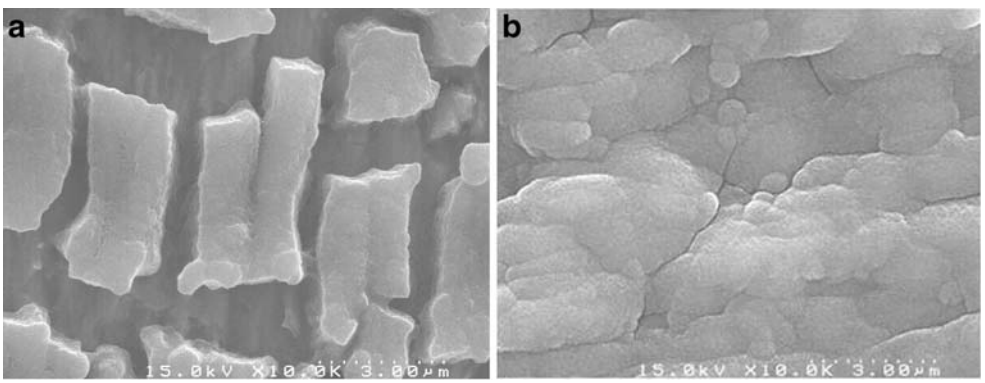

Fig. 9 Scanning electron microscope (*SEM*) images for bare Si thin film (**a**) and fullerene-coated Si thin film electrodes (**b**) after the 30th cycles

silicon thin films demonstrates no such surface cracking because of the presence of the polymeric fullerene layer. It is reasonable to say that the polymeric layer can suppress the propagation of the cracks in the initial cycling. The polymeric layer contributed to stabilize the Si surface, so the cracking as the result of the volume change can be significantly reduced. Therefore, the fullerene-coated silicon thin film anodes performed excellent cycling stability over the Si thin film anodes as seen in Fig. 6.

Conclusions

In this work, the chemical structure and electrochemical performances of fullerene-coated silicon thin films as anode materials for rechargeable lithium batteries have been studied and then compared with those of the bare Si thin film case. HRTEM, Raman spectroscopy, and XPS results have shown that the fullerene-coated silicon thin film is a polymeric film with amorphous and disordered graphitic structure. The presence of the polymerized fullerene films leads to improving the electrochemical performance by means of enhancing the cyclic stability, and the capacity retention is also improved significantly. This is attributed to the better kinetic property at the interface of the electrode and the electrolyte, as confirmed by impedance analysis. In addition, experimental results have shown the vital role of polymerized fullerene films, and these findings are quite important for the modification of silicon or other metal type anodes, which are commonly subject to mechanical degradation.

Acknowledgment This research was supported by a grant from the 'Center for Nano-structured Materials Technology' under '21st century Frontier R&D Programs'of the Ministry of Science and Technology, Republic of Korea. The preparations of silicon thin films were prepared by Seok Min Moon.

References

1. Poizot P, Laruelle S, Grugeon S, Dupont L, Tarascon JM (2000) Nature 407:496. doi:10.1038/35035045
2. Besenhard JO, Besenhard T (eds) (1999) Handbook of battery materials. Wiley-VCH, Weinheim
3. Nishi Y (2001) J Power Sources 100:101–106. doi:10.1016/S0378-7753(01)00887-4
4. Bitsche O, Gutmann G (2004) J Power Sources 127:8–15. doi:10.1016/j.jpowsour.2003.09.003
5. Fellner C, Newman J (2000) J Power Sources 85(2):229–236. doi:10.1016/S0378-7753(99)00344-4
6. Tarascon JM, Grugeon S, Morcrette M, Laruelle S, Rozier P, Poizot P (2005) C R Chimie 8(1):9–15
7. Aurbach D (2005) J Power Sources 146(1–2):71–78. doi:10.1016/j.jpowsour.2005.03.151
8. Li G, Lu G, Huang B, Huang H, Xue R, Chen L (1995) Solid State Ion 81:15. doi:10.1016/0167-2738(95)00166-4
9. Obrovac MN, Christensen L (2004) Electrochem Solid-State Lett 7:A93. doi:10.1149/1.1652421
10. Huggins RA (1998) Solid State Ion 113–115:57–67. doi:10.1016/S0167-2738(98)00275-6
11. Yoshio M, Wang H, Fukuda K, Umeno T, Dimov N, Ogumi Z (2002) J Electrochem Soc 149(12):A158–A1603. doi:10.1149/1.1518988
12. Beaulieu Y, Eberman KW, Turner RL, Krause LJ, Dahn JR (2001) J Electrochem Solid-State Lett 4:A137. doi:10.1149/1.1388178
13. Beaulieu Y, Bonakdarpour A, Hatchard TD, Fleischauer MD, Dahn JR (2002) J Electrochem Soc 149:A1598. doi:10.1149/1.1518988
14. Kasavajjula U, Wang CS, Appleby AJ (2007) J Power Sources 163(2):1003–1039. doi:10.1016/j.jpowsour.2006.09.084
15. Chen LB, Xie JY, Yu HC, Wang TH (2008) Si–Al thin film anode material with superior cycle performance and rate capability for lithium ion batteries. Electrohim Acta 53:8149–8153. doi:10.1016/j.electacta.2008.06.025
16. Kim JB, Lee HY, Lee KS, Lim SH, Lee SM (2003) Electrochem Commun 5(7):544–548. doi:10.1016/S1388-2481(03)00120-6
17. Chiu KF, Lin KM, Lin HC, Hsu CH, Chen CC, Shieh DT (2008) J Electrochem Soc 155(9):A623–A627. doi:10.1149/1.2948357
18. Arie AA, Vovk OM, Song JO, Cho BW, Lee JK (2009) Carbon film covering originated from fullerene C_{60} on the surface of lithium metal anode for lithium secondary batteries. J Electroceram. doi:10.10071/s10832-008-9413-6
19. Eklund PC, Zhou P, Wang KA, Dresselhaus MS, Dresselhaus G (1992) J Phys Chem Solids 53(11):1391. doi:10.1016/0022-3697(92)90234-5
20. Persson PA, Edlund U, Jacobsson P, Johnels D, Soldatov A, Sunqvist B (1999) Chem Phys Lett 258:540. doi:10.1016/0009-2614(96)00743-9
21. Maccario M, Croguennec L, Desbat B, Couzi M, Le Cras F, Servant L (2008) J Electrochem Soc 155(12):A882
22. Laspade P, Marchand A, Couzi M, Cruege F (1984) Carbon 22:375. doi:10.1016/0008-6223(84)90009-5
23. Yoon SF, Rusli H, Ahn J, Zhang Q (1998) Vacuum 49(1):67. doi:10.1016/S0042-207X(97)00136-X
24. Chakrabarti K, Basu M, Chaudhuri S, Pal AK, Hanzawa H (1999) Vacuum 53:870. doi:10.1016/S0042-207X(98)00409-6
25. Robertson J (2002) Mater Sci Eng 37:129. doi:10.1016/S0927-796X(02)00005-0
26. Vazquez RP, Brain RA, Ross D, Yeh NC (1992) Surf Sci Spectra 1:242. doi:10.1116/1.1247645
27. Ramm M, Ata M, Gross T, Unger W (2000) Appl Phys A 70:388. doi:10.1007/s003390051053
28. Hatchard TD, Dahn JR (2004) J Electrochem Soc 151(6):A838–A842. doi:10.1149/1.1739217
29. He BL, Dong B, Li HL (2007) Electrochem Commun 9:425
30. Yang SB, Song HH, Chen XH (2006) Electrochem Commun 8:137